

Supporting Information

Nucleation, Growth, and Repair of a Cobalt-Based Oxygen Evolving Catalyst

Yogesh Surendranath, Daniel A. Lutterman, Yi Liu and Daniel G. Nocera*

*Department of Chemistry, 6-335, Massachusetts Institute of Technology, Cambridge,
Massachusetts 02139-4307*

nocera@mit.edu

<i>Index</i>	<i>Page</i>
Experimental methods	S2-S5
Fig. S1. Normalized chronoamperograms at a variety of step voltages	S7
Fig. S2. $1 \times 1 \mu\text{m}$ AFM images of catalyst nucleation	S8
Fig. S3. Koutecký-Levich plots of catalyst growth	S9
Fig. S4. Dependence of Tafel behavior for catalyst growth on Co^{2+} concentration	S10
Fig. S5. pH dependence of Tafel behavior for catalyst growth	S11
Fig. S6. MeP_i concentration dependence of Tafel behavior for catalyst growth	S12
Fig. S7. Calibration curves for Co^{2+} induced ^{31}P -NMR line broadening	S13

Experimental Methods

Materials. $\text{Co}(\text{NO}_3)_2$ 99.999% was used as received from Aldrich or Strem. KOH 88%, KNO_3 , KH_2PO_4 , acetic acid and boric acid were reagent grade and used as received from Mallinckrodt. Methylphosphonic acid 98% (Aldrich) was recrystallized from boiling acetonitrile (HPLC grade, Aldrich) prior to use. All electrolyte solutions were prepared with reagent grade water of >18 $\text{M}\Omega\text{-cm}$ resistivity (Ricca Chemical or Millipore Type 1).

General Electrochemical Methods. All electrochemical experiments were conducted using a CH Instruments 760C or 760D potentiostat, a BASi Ag/AgCl reference electrode, and a high surface Pt-mesh counter electrode. Rotating disk electrode measurements were conducted using a Pine Instruments MSR rotator. All electrochemical experiments were performed using a three-electrode electrochemical cell with a porous glass frit separating the working and auxiliary compartments. Unless otherwise stated, all experiments were performed at ambient temperature (22 ± 2 $^\circ\text{C}$) and electrode potentials were converted to the NHE scale using $E(\text{NHE}) = E(\text{Ag}/\text{AgCl}) + 0.197$ V.

Solution Preparations. In all cases, electrolyte solutions were prepared by diluting appropriate amounts of stock solutions of 10 mM Co^{2+} , 2.5 M KNO_3 and 1 M MeP_i with reagent grade water. To prevent the precipitation of cobalt ions, the Co^{2+} stock solution was never added directly to the concentrated 1 M MeP_i stock solution. For all Tafel data collections, solutions of the desired composition were permitted to equilibrate for ca. 1 h prior to the experiment.

Potential Step Chronoamperometry. Potential step chronoamperometry (CA) traces were recorded in quiescent solution using a 3 mm diameter glassy carbon disk button electrode (CH Instruments) polished to a mirror shine for 60 sec with 0.05 μm alumina (CH Instruments) and sonicated for 60 sec in reagent grade water prior to each experiment. The electrode was initially polarized at 0.75 V for 100 sec, during which time only double-layer charging occurred. Then, the electrode was stepped for 100 sec to various potentials sufficient for catalyst nucleation under these conditions (Figure 1). In all cases, data points were sampled every 0.01 sec. Over numerous independent experiments using the same potential step parameters the values of j_{max} and t_{max} were found to be reproducible to within 5%.

AFM Imaging of Catalyst Nucleation. AFM studies were conducted using highly oriented pyrolytic graphite (HOPG) electrodes (Grade SPI-2, SPI Supplies) that were prepared by cleaving a thin layer of HOPG from a bulk slab using double-sided Scotch tape and mounting onto a glass slide. HOPG electrodes prepared in this fashion were contacted using a toothless alligator clip and immersed in the solution such that a 0.1-0.15 cm^2 area of the HOPG surface was exposed to the electrolyte. Catalyst islands were partially nucleated from quiescent solution onto the HOPG surface using potential step chronoamperometry with a step potential of 0.97 V. As above, the electrodes were held at 0.75 V for 100 sec prior to initiation of the potential step. These potential step conditions gave rise to an average t_{max} of 10.1(1) s. Thus, for electrolysis

times of 0.2, 0.5 and $1 \times t_{max}$, electrolysis was terminated after ca. 2, 5 and 10 sec respectively. For longer electrolysis times, the amperometric trace was monitored and electrolysis was manually terminated at the appropriate time relative to the observed t_{max} in each run. This procedure served to limit errors due to slight variations (< 2 sec) in the absolute value of t_{max} between independent experiments. In all cases, after termination of electrolysis, the electrode was immediately removed from solution, rinsed in reagent water, and dried in preparation for imaging by AFM.

AFM images were collected using a Veeco Nanoscope Dimension 4100 (Veeco Instruments Inc., Santa Barbara, CA) operating in tapping mode with a Veeco silicon nitride probe with a resonance frequency of ~ 200 KHz and average tip radius of 3 nm. All measurements were performed in air and at room temperature. Percent coverage values were determined using Nanoscope V5.31 software.

Tafel Data Collection. Activation controlled current-potential data (Figures 3 and S4-S6) were obtained by conducting controlled potential electrolyses for film formation under the appropriate electrolyte conditions at a wide variety of applied potentials and rotation rates onto a 5 mm diameter (0.20 cm^2) Pt rotating disk electrode. Prior to each Tafel run, the electrode was polished to a mirror shine with $0.05 \text{ }\mu\text{m}$ alumina and sonicated for 60 sec in reagent grade water. To eliminate the impact of nucleation on the kinetics of steady-state catalyst growth, a 200 sec galvanostatic pulse at $50 \text{ }\mu\text{A}/\text{cm}^2$ was applied to the electrode, rotated at 2500 rpm, prior to the initiation of Tafel data collection. This pulse corresponds to $10 \text{ mC}/\text{cm}^2$ charge passed for deposition, which is ~ 10 fold higher than the typical charge passed at $8 \times t_{max}$ ($< 1 \text{ mC}/\text{cm}^2$) in the nucleated growth studies, ensuring that the catalyst film completely covers the Pt surface. Following this initial deposition, the potential of the electrode was swept from low to high values, in 10 mV increments, across the linear Tafel region. At each potential value, the current was permitted to reach a steady-state for 50-200 sec while the electrode was rotated at 2500 rpm. Following this period of time, the rotation rate was decremented to 1600, 1111, 825 and 625 rpm. At each rotation rate, the current was permitted to stabilize for 20 sec. Following each sweep of rotation rates, the potential was incremented and the current was again permitted to reach a steady-state at a 2500 rpm rotation speed before the sequence was repeated. The pH was continuously monitored during Tafel data collection with a pH probe (VWR) positioned in the working compartment, and the pH was held at the designated value within 0.02 units with periodic addition of 1-2 μL of concentrated KOH as needed. Importantly, KOH was only added at the beginning of a new potential step rather than during the sweep of rotation rates to minimize the impact of transient current spikes resulting from base addition from convoluting the subsequent Koutecký-Levich analysis. The solution in the working compartment was stirred gently during Tafel data collection to prevent the formation of large concentration gradients and allow efficient mixing of any added KOH.

Following Tafel data collection, the inverse of the steady state current density values (j^{-1}) were plotted versus $\omega^{-1/2}$ to yield Koutecký-Levich plots for each potential as shown in Figure S3.

Koutecký-Levich plots were found to be linear over the entire potential range and extrapolation of these plots to infinite rotation rate ($\omega^{-1/2} = 0$) yielded the activation-controlled current density values, j_{ac} , at each potential (Figures 3 and S4-S6). In all cases, ohmic potential losses due to uncompensated solution resistance were found to be less than 1 mV and were ignored.

Co²⁺ Concentration Dependence. The dependence of catalyst formation rate on Co²⁺ concentration was assessed by collecting Tafel plots, using the procedure described above, from solutions containing 0.1, 0.18, 0.32, 0.56 and 1 mM Co²⁺ (Figure S4). In all cases, the electrolyte conditions were 0.02 M MeP_i, 1.97 M KNO₃, pH 7.5. The data were interpolated at potential values of 1.04, 1.06, 1.08, and 1.1 V, which cut across the linear Tafel region of all plots, to yield the dependence of j_{ac} on Co²⁺ concentration (Figure 4).

pH Dependence. The dependence of catalyst formation rate on pH was assessed by collecting Tafel plots, using the procedure described above, at pH 7.00, 7.25, 7.49, 7.73, 7.98 and 8.25 (Figure S5). In all cases, the electrolyte conditions were 0.4 mM Co²⁺, 0.02 M MeP_i, 1.97 M KNO₃. The data were interpolated at values of $\log(j_{ac}) = -5.5, -5.0, -4.5$, and -4.0 , which cut across the linear Tafel region of all plots, to yield the dependence of the required potential on pH (Figure 5).

Phosphate Concentration Dependence. The dependence of catalyst formation rate on MeP_i concentration was assessed by collecting Tafel plots, using the procedure described above, at [MeP_i] = 178, 100, 56.2, 31.6, 17.8, 10.0, 5.6, 3.2, 1.8, and 1 mM (Figure S6). All solutions were held at pH 7.5 and 2 M ionic strength, with KNO₃ background electrolyte, and contained 0.4 mM Co²⁺. The data were interpolated at values of $\log(j_{ac}) = -5.0, -4.5$, and -4.0 , which cut across the linear Tafel region of all plots, to yield the dependence of the required potential on MeP_i concentration (Figure 6).

Computation of Equilibrium Constants and Co²⁺ Speciation. Using specific ion interaction theory (SIT),¹ as implemented in the program *Ionic Strength Corrections using Specific Interaction Theory*, Version 2.0,² relevant equilibrium constants were calculated for Co²⁺ and MeP_i species in solution under the 2 M ionic strength conditions, KNO₃ background electrolyte, employed in this study. The reported first and second pK_a values of methylphosphonic acid at 0.1 M ionic strength are 2.10 and 7.51 respectively.³ These values were corrected using the cation SIT parameter for H⁺, 0.07, and the anion SIT parameters for MePO₃H⁻ and MePO₃²⁻ surrogates, H₂PO₄⁻, -0.14, and HPO₄²⁻, -0.10, respectively. This yielded corrected values of pK_{a1} = 1.7 and pK_{a2} = 7.0. The measured formation constant for Co(MePO₃) is $\log(K) = 2.24$ at 0.1 M ionic

(1) Grenthe I.; Plyasunov A. *Pure Appl. Chem.* **1997**, 69, 951-958.

(2) *Ionic Strength Corrections using Specific Interaction Theory*, Version 2.0; Pettit L. D.; Puigdomenech I.; Wanner H.; Sukhno I.; Buzko V. ©IUPAC 2004

(3) Sigel, H.; Da Costa, C. P.; Song, B.; Carloni, P.; Gregáň, F. *J. Am. Chem. Soc.* **1999**, 121, 6248-6257.

strength.⁴ This value was corrected using the cation SIT parameter for Co^{2+} , 0.14, and the anion SIT parameter for the MePO_3^{2-} surrogate, HPO_4^{2-} , -0.10, to yield a value of $\log(K) = 1.4$. Using these values, the speciation of 0.4 mM Co^{2+} as a function of MeP_i concentration was computed at pH 7.5 using ChemEQL, version 3.1,⁵ to determine that 50% of the Co is bound at an MeP_i concentration of 50 mM. The first pK_a of $\text{Co}(\text{OH})_2$ is 8.9 at 0.1 M ionic strength,⁶ corresponding for a formation constant for $\text{Co}(\text{OH})^+$ from OH^- and Co^{2+} of $\log(K) = 5.1$. Using the cation SIT parameter for Co^{2+} , 0.14, the anion SIT parameter for OH^- , 0.09, and the estimated SIT parameter for $\text{Co}(\text{OH})^+$, 0.15, a corrected value of $\log(K) = 4.8$ was obtained, corresponding to a corrected pK_a of 9.2.

Catalyst Dissolution Studies. Catalyst dissolution studies employed working electrodes consisting of fluorine-tin-oxide coated glass (FTO; TEC-7) with $7\ \Omega/\text{sq}$ surface resistivity which were purchased as pre-cut $1\ \text{cm} \times 2.5\ \text{cm}$ glass pieces from Hartford Glass. These FTO-coated glass pieces were rinsed with acetone and water prior to use in all catalyst dissolution experiments and a $\sim 0.5\ \text{cm}$ wide strip of Scotch tape was affixed to the FTO coated side such that a $1\ \text{cm}^2$ area was exposed to solution. Catalyst films were then prepared on these electrodes via controlled-potential electrolysis of 0.1 M phosphate electrolyte, pH 7.0, containing 0.5 mM Co^{2+} . In all cases, electrodepositions were carried out on quiescent solutions at 1.05 V with passage of $100\ \text{mC}/\text{cm}^2$. At this deposition potential, negligible water oxidation catalysis is observed.⁷ Thus, the $100\ \text{mC}/\text{cm}^2$ charge passed provides an accurate estimate of the Co content of the film, $\sim 1\ \mu\text{mol}\ \text{Co}/\text{cm}^2$. Following electrodeposition, the catalyst film coated electrode was rinsed with reagent grade water and placed in a 20 mL bath of stirred Britton-Robinson buffer (0.04 M borate, 0.04 M phosphate and 0.04 acetate) of the appropriate pH and operated at either 1 or 0 mA/cm^2 . Small aliquots (0.5 mL) of the electrolyte solution were sampled every 15 min for the 1 h duration of each experiment.

Following each experiment, the Co^{2+} concentration in each aliquot was quantified by measuring the full-width at half maximum (FWHM) of the ^{31}P NMR signal for phosphate in the electrolyte. The paramagnetism of the high spin Co^{2+} ion induces line broadening in the ^{31}P NMR signal, the magnitude of which is directly proportional to the Co^{2+} concentration. Thus, the measured FWHM values for this signal in each aliquot were compared to a standard curve to determine the concentration of Co^{2+} . Representative calibration curves for pH 4 and pH 7 are shown in Figure S7. Since the breadth of the ^{31}P NMR signal is highly sensitive to instrumental variables, data for the calibration curves were recorded alongside the experimental samples in all cases. Additionally, as seen in Figure S7, the Co^{2+} -induced line broadening is highly pH dependent; thus, separate calibration curves were recorded at each pH interrogated. Using the measured Co^{2+}

(4) Sigel, H.; Chen, D.; Corfu, N. A.; Gregan, F.; Holy, A.; Strassak, M. *Helv. Chim. Acta* **1992**, 75, 2634-2656.

(5) ChemEQL, Version 3.1; Müller, B; Limnological Research Center EAWAG/ETH; Switzerland

(6) Chaberek, S.; Courtney, R. C.; Martell, A. E. *J. Am. Chem. Soc.* **1952**, 74, 5057-5060.

(7) Surendranath, Y.; Dincă, M.; Nocera, D. G. *J. Am. Chem. Soc.* **2009**, 131, 2615-2620.

concentrations and the volume of solution in the working compartment of the electrolysis cell the molar quantity of Co ions leached was determined for each data point. These values were divided by the $\sim 50 \mu\text{M Co}^{2+}$ concentration expected for complete catalyst dissolution into the 20 mL electrolyte solution to determine the fraction dissolved, f , at each time point (Figure 7). The fraction dissolved after 1 h is shown versus pH in Figure 8.

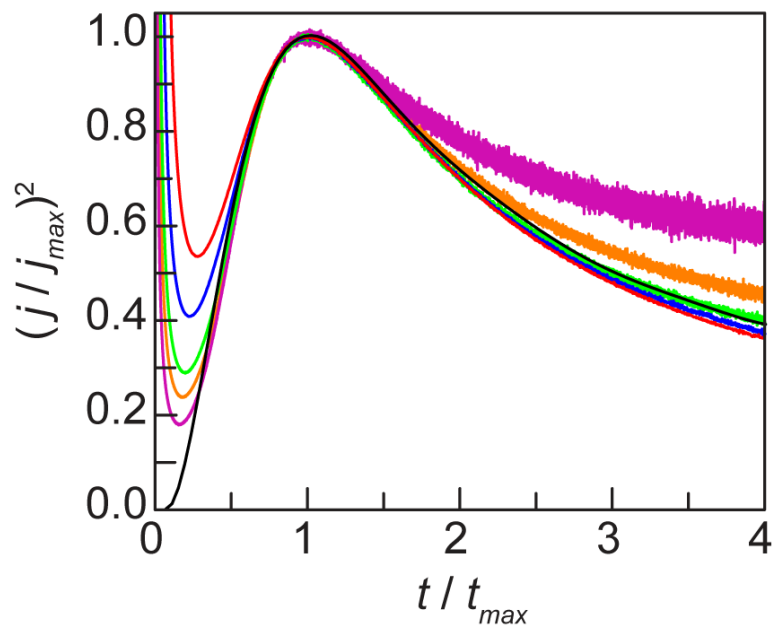


Figure S1. Normalized potential step chronoamperograms of a freshly polished glassy carbon disk electrode recorded in 0.4 mM Co^{2+} and 0.02 M MePi, 1.97 M KNO_3 electrolyte at pH 7.5. Data recorded with a step voltage of 1.01(—), 0.99(—), 0.97(—), 0.95(—), and 0.93(—) V following a 100 sec pulse at 0.75 V (not shown). Theoretical normalized chronoamperogram for progressive nucleated growth with a 4th (—) order nucleation rate law.

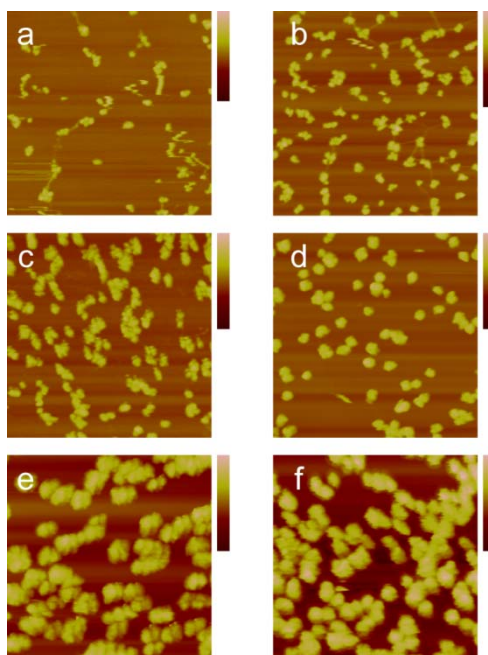


Figure S2. Representative $1 \times 1 \mu\text{m}$ AFM images of a highly oriented pyrolytic graphite electrode after being subjected to potential step polarization from 0.75 to 0.97 V for ca. (a) 0.2, (b) 0.5, (c) 1, (d) 2 (e) 4, and (f) $8 \times t_{\text{max}}$ (10.1(1) s). Bars to the right of each image indicate the depth with a full scale value of (a) 20, (b) 30, (c) 50, (d) 75, (e) 75 and (f) 50 nm. Electrolyte conditions: 0.4 mM Co^{2+} and 0.02 M MePi , 1.97 M KNO_3 electrolyte at pH 7.5 (2 M ionic strength).

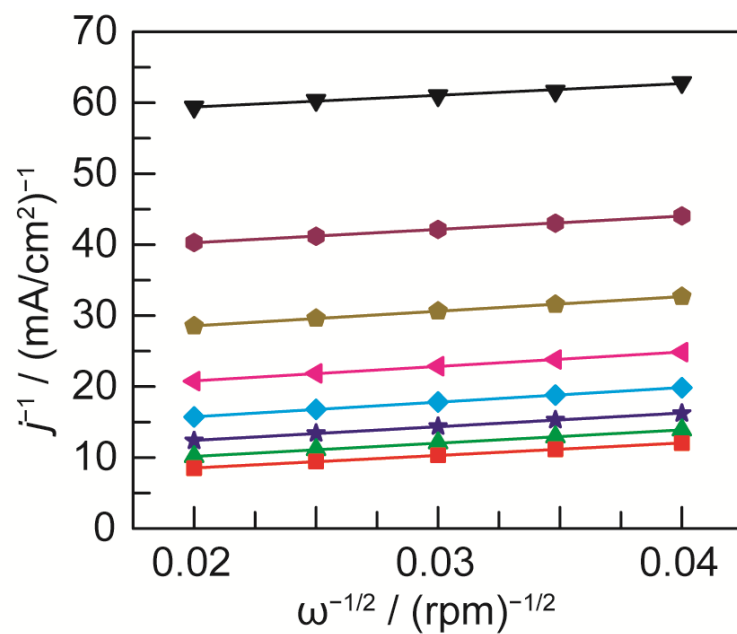


Figure S3. Koutecký-Levich plots of Co-OEC catalyst film formation from 0.4 mM Co^{2+} and 0.02 M MeP_i , 1.97 M KNO_3 electrolyte at pH 7.5 at applied potentials of 0.87 (▼), 0.88 (◆), 0.89 (◆), 0.90 (◀), 0.91 (◆), 0.92 (★), 0.93 (▲), and 0.94 (■) V.

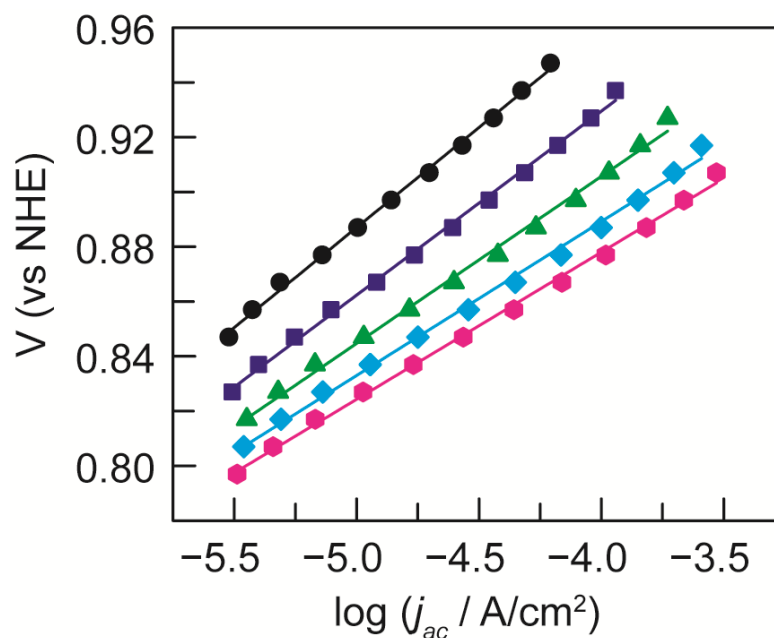


Figure S4. Tafel plots of Co-OEC catalyst film formation from 0.02 M MeP_i, 1.97 M KNO₃ electrolyte at pH 7.5 containing of 0.1 (●), 0.18 (■), 0.32 (▲), 0.56 (◆) and 1 (◆) mM Co²⁺. Activation controlled current density values (j_{ac}) were derived from Koutecký-Levich analysis of steady-state current densities measured at multiple rotation rates, as in Figure S3. Average Tafel slope is 62(8) mV/decade.

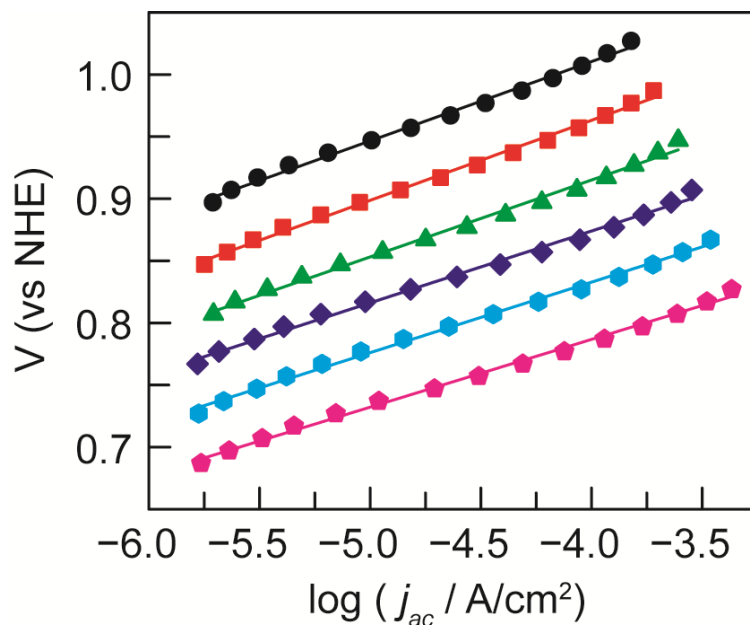


Figure S5. Tafel plots of Co-OEC catalyst film formation from 0.4 mM Co^{2+} and 0.02 M MePi , 1.97 M KNO_3 electrolyte at pH 7.00 (●), 7.25 (■), 7.49 (▲), 7.73 (◆), 7.98 (⬢) and 8.25 (⬠). Activation controlled current density values (j_{ac}) were derived from Koutecký-Levich analysis of steady-state current densities measured at multiple rotation rates, as in Figure S3. Average Tafel slope is 60(4) mV/decade.

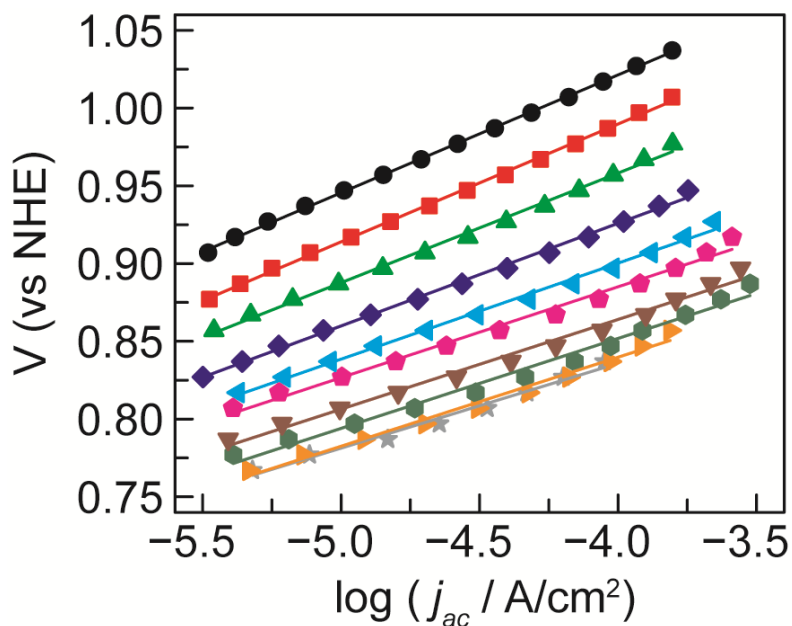


Figure S6. Tafel plots of Co-OEC catalyst film formation from a 0.4 mM Co^{2+} at pH 7.5 electrolyte solution containing 178 (●), 100 (■), 56.2 (▲), 31.6 (◆), 17.8 (◄), 10 (◆), 5.6 (▼), 3.2 (●), 1.8 (▶), and 1 (★) mM MePi. All solutions were held at 2 M ionic strength with an appropriate amount of KNO_3 . Activation controlled current density values (j_{ac}) were derived from Koutecký-Levich analysis of steady-state current densities measured at multiple rotation rates, as in Figure S3. Average Tafel slope is 64(8) mV/decade.

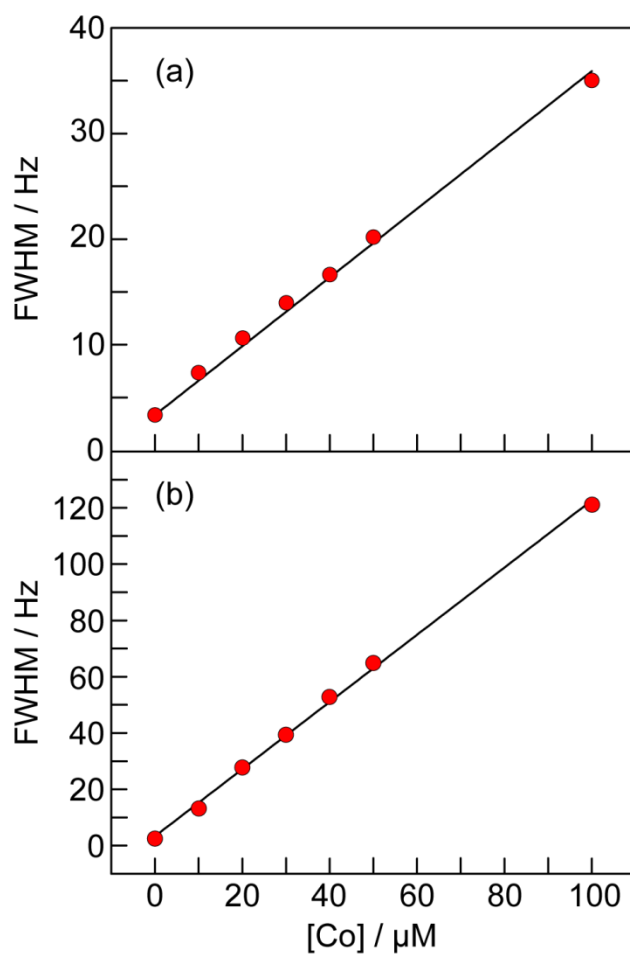


Figure S7. Representative calibration curves for the full-width at half maximum (FWHM) of the ^{31}P -NMR line of inorganic phosphate versus Co^{2+} concentration at (a) pH 4 and (b) pH 7.